Bull Mater Sci (2021)44:2
https://doi.org/10.1007/s12034-020-02292-3

Decolourization of rhodamine B and methylene blue dyes in the presence of bismuth tungstates: a detailed investigation on the effect of grain size

SHOMAILA KHANAM and SANJEEB KUMAR ROUT*
Department of Physics, Birla Institute of Technology, Ranchi 835215, India
*Author for correspondence (skrout@bitmesra.ac.in)

MS received 18 June 2020; accepted 6 August 2020

Abstract. Solid-state reaction method was opted for the preparation of bismuth tungstates (Bi_2WO_6) in the stoichiometric ratio. The structural characterization related that the material has got orthorhombic symmetry. The high-energy ball milling did not show any structural change, but a reduction in grain size was observed from 100 to 34 nm after 5 h. The higher activity for the decolourization of rhodamine B (RHB) and methylene blue (MB) in the presence of UV light has been studied by employing Bi_2WO_6 as a catalyst. The dye degradation was observed by a decrease in the absorption spectrum and decolourization in the presence of UV irradiation. The degradation efficiency was found to be dependent on the size of the catalyst added in the dye solution, which may be due to increased surface area that increased the number of active sites for the reaction. The degradation efficiency of the unmilled and 5-h ball milled (Bi_2WO_6) catalyst was observed to be 32 and 90% in RHB, respectively. While in MB, 24 and 49% degradation efficiency was achieved by unmilled and 5-h ball milled (Bi_2WO_6) catalyst. The degradation rate coefficient was found to be in the decreasing order of RHB > MB, which pursued the first-order kinetic mechanism. Therefore, Bi_2WO_6 can act as a catalyst for the treatment of noxious and imperishable organic pollutants in water.

Keywords. XRD; photocatalysis; degradation; rhodamine B; methylene blue.

1. Introduction

Textile industries cause the most precarious problem of water pollution due to the dumping or discharging of dye wastewater into water bodies. In India, river pollution has crossed the mark of crisis due to improper arrangement for disposal of wastewater or due to the non-availability of advanced technological material for dye degradation. Non-biodegradable materials and toxic dyes are continuously disposed in the river, thus rendering toxic water and making it unfit for further use. The organic dyes cause severe environmental and biological problems, also induces irritation to human eyes and skin. It has been reported that rhodamine B (RHB) causes DNA damage [1], methylene blue (MB) causes sperm motility leading to infertility issues [2], and methyl orange shows mutagenic properties [3].

Transition metal tungstates are inorganic materials that have significant applications in fluorescent lamps [4,5], microwave [6], as scintillators [7,8], as laser host materials [9,10], magnetic materials [11], oxide ion conductors [12], humidity sensors [13] and as a catalyst [14–17]. Bismuth tungstates belong to the family of cation-deficient aurivillus phases, which act as a heterogeneous photocatalyst for degrading azo dyes. It gives rise to an electron–hole pair that participates in the redox reaction in photocatalysis, thus ultimately leading to the decomposition of persistent organic pollutants under visible and UV light irradiation [18–20].

It is reported that nanocomposites of Bi_2WO_6 prepared through hydrothermal technique could degrade RHB up to 9.68% and MB up to 10.77% in 75 min [21]. Another literature reported that Bi_2WO_6 mixed with C_{60} degraded MB up to 80% in 2 h [22]. Whereas nanosheets of Bi_2WO_6 prepared through the hydrothermal method maintained at pH 8 degraded 37% of MB in 22 h and 28% of RHB in 280 min [23]. The uncalcined flower-like Bi_2WO_6 superstructure prepared by hydrothermal method degraded 84% of RHB in 60 min and flower-like calcined Bi_2WO_6 degraded 97% of RHB in 60 min [24]. Bi_2WO_6, prepared by above techniques have got the limitations to produce the photocatalyst in bulk and thus may not be suitable for industries where large amount of photocatalyst are required. These techniques involve various chemicals that are not eco-friendly and cost-effective. In this study, Bi_2WO_6 has been prepared through solid-state reaction route, and the size reduction is made through the ball milling technique, thus making the overall experiment cost-effective, toxic-free and appropriate for mass production of the photocatalyst.

Published online: 03 February 2021

2. Experimental

2.1 *Synthesis of Bi_2WO_6*

The cost-effective solid-state reaction technique was opted for the synthesis of Bi_2WO_6 ceramics. The stoichiometrically calculated Bi_2O_3 and WO_3 were thoroughly ground in the liquid medium using an agate mortar for 6 h. The powder mixture then calcined at 800°C for 6 h and 900°C for 4 h with an intermediate grinding in a wet medium. Phase purity was checked using a standard X-ray diffractometer (XRD; Smart Lab, Rigaku, Japan). The monophasic Bi_2WO_6 ceramic was grounded for 5 h in liquid medium using a planetary ball milling unit. Powder to ball ratio was kept to be 1:10. The milling speed was maintained at 200 rpm. The ball-milled sample was dried using an infrared lamp. Phase stability after ball milling was re-examined using an XRD and Fourier transform infrared (FTIR) spectrometer. FTIR spectra were examined in the frequency range 400 to 4000 cm^{-1} in the presence of KBr, as a diluting agent. The surface area was calculated using a standard BET (Nova touch-LX1, Quantachrome). The photocatalytic test was performed in a self-designed photoreactor chamber, which was installed with UV lamps. The degradation rate of dyes (RHB and MB) was calculated from the absorption graph, which was recorded by a Ultra violet and visible spectrometer (Lambda 35, Perkin-Elmer, USA). For the photocatalytic test, 5 ppm of dye solution was prepared using de-ionized water. A quantity of 100 ml of dye solution was taken in a Pyrex glass beaker, and 20 mg of Bi_2WO_6 catalyst was added. The dye-catalyst mixture was continuously stirred for 1 h using a magnetic stirrer, heated at 40°C rotating at a speed of 250 rpm in the dark so that dye molecule gets perfectly adsorbed on the photocatalyst's surface. The absorption spectra of the photocatalyst in dye solution for 1 h without UV irradiation showed negligible change after 1 h, suggesting that there is no change in dye concentration. The beaker with dye and photocatalyst was kept in the photocatalytic chamber with UV irradiation of power 72 watts. The distance between the sample and the UV lamps was maintained to be 13 cm. After every 1 h interval, 3–5 ml of aliquots were taken out and centrifuged (Remi PR-24) and examined under UV–vis spectrometer.

3. Results and discussion

3.1 *Structural analysis*

Figure 1 shows the XRD pattern of bismuth tungstate powder obtained before and after ball milling for 5 h. The X-ray diffractograph shows the orthorhombic symmetry of the ceramic and matches with the JCPDS card no-79-2381) very well. The monophasic nature of Bi_2WO_6 before and after ball milling can be seen from the diffractogram. The

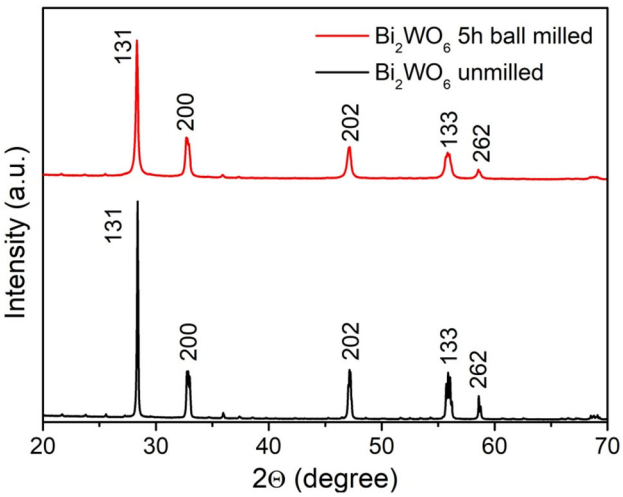

Figure 1. XRD diffractograph of Bi_2WO_6 unmilled and 5 h ball-milled samples.

diffraction peaks became gradually broader with ball milling, thus showing that ball milling decreases the average crystallite size. The average crystallite size of the unmilled Bi_2WO_6 was 100 nm, while 5 h ball milling reduced its crystallite size to 34 nm as calculated by using Scherrer's formula.

Figure 2a shows the FTIR spectra of Bi_2WO_6 before and after ball milling within the frequency range of 1000–400 cm^{-1}. The leading absorption bands at 501 and 709.5 cm^{-1} represent the stretching vibration mode of Bi–O and W–O bond, respectively [25–30]. These band positions remain unchanged after 5 h ball milling suggesting no change in crystal symmetry.

The experimental Raman spectra of unmilled and 5 h ball-milled Bi_2WO_6 at room temperature are shown in figure 2b. Both the spectra exhibit a similar profile, suggesting no changes associated with the decrease in the size of Bi_2WO_6 due to ball milling. All the characteristic peaks of Bi_2WO_6 were identified as being in the range of 200 to 1000 cm^{-1} [31]. The active modes at 792.94 and 828.58 cm^{-1} are an indication of bismuth tungstate and may be credited to the antisymmetric modes and symmetric modes of the O–W–O bonds [32]. The peak at 721.83 cm^{-1} explicates the linking mode of tungstates [33,34]. The vibration at 334.46 cm^{-1} was allocated to WO_2 mode [35,36]. The peak at 307.23 cm^{-1} is associated with the simultaneous motion of Bi^{3+} and WO_6^{6-} along the crystal lattice [31,32].

3.2 *Optical properties*

The optical bandgap was calculated by Kubelka–Munk equation and presented in figure 3a. The Kubelka–Munk function is represented by the equation $[F(R)hv]^{1/n} = C_1(E_{gap} - hv)$, where $F(R)$ is the Kubelka–Munk function, hv the energy of a photon and C_1 the proportionality constant [37–40]. The optical energy bandgap of Bi_2WO_6

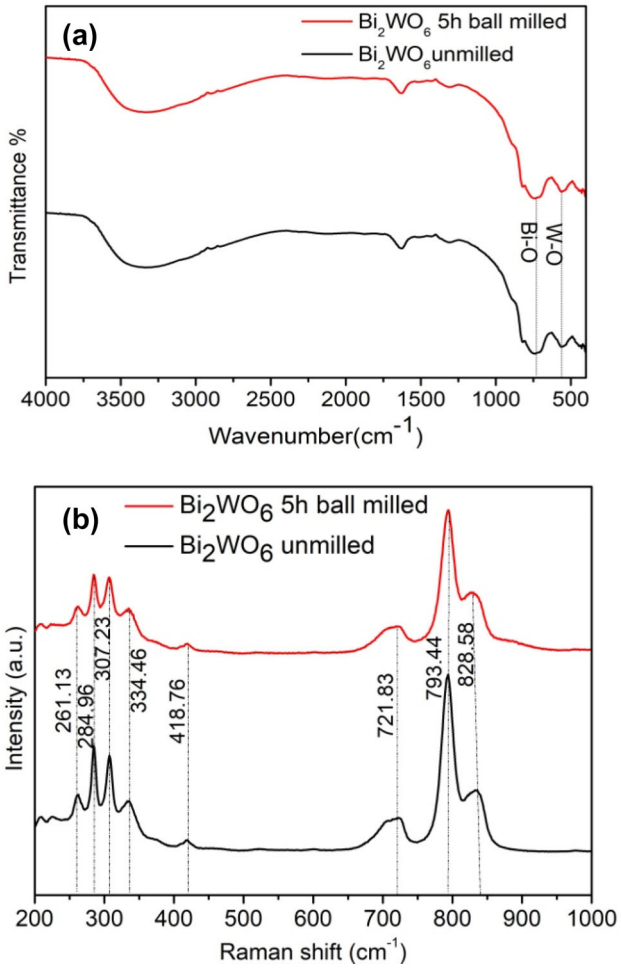

Figure 2. (**a**) FTIR and (**b**) Raman spectra of Bi_2WO_6 (unmilled) and 5 h ball-milled samples.

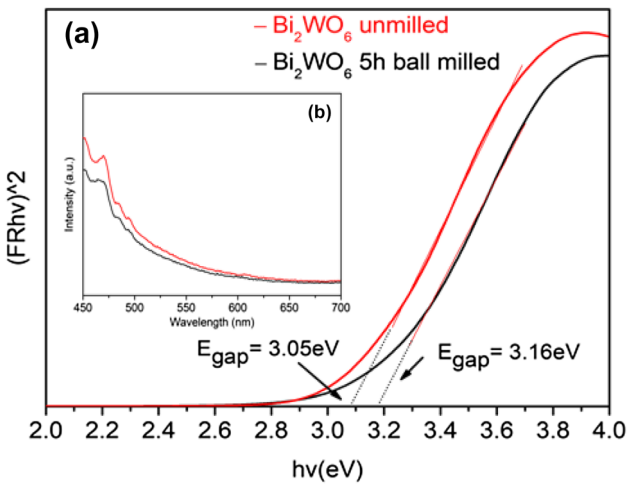

Figure 3. (**a**) The optical bandgap of unmilled and 5 h ball-milled Bi_2WO_6 powder at room temperature. Inset (**b**) shows the fluorescence spectra of the respective powders.

unmilled and Bi_2WO_6 5 h ball-milled was found to be 3.05 and 3.16 eV, respectively, determined by tauc plot, as shown in figure 3a.

The photoluminescence (PL) emission spectra were carried to investigate the recombination rate of photoexcited charge carriers. Figure 3 (inset) shows PL spectra of Bi_2WO_6 unmilled and 5 h ball-milled powders. The weaker PL intensity of Bi_2WO_6 5 h ball-milled indicates a lower recombination rate of photogenerated electron–hole pairs [41]. The photocatalytic result discussed subsequently is also in accordance with PL result, indicating higher photocatalytic effect in Bi_2WO_6 5 h ball-milled sample allowing the lower rate of holes and electrons recombination.

3.3 *Degradation of RHB*

The photocatalytic activity of an unmilled and 5 h ball-milled Bi_2WO_6 catalyst was performed by degrading RHB under ultraviolet light. RHB has maximum absorption at 554 nm. It does not show stability under UV irradiation and is degraded by 27% in 15 h of UV irradiation. The absorption spectra of RHB under 15 h of UV–vis irradiation is shown in figure 4a. RHB is more easily adsorbed by 5 h ball-milled Bi_2WO_6 than by unmilled Bi_2WO_6, illustrated in figure 4b and c. The higher removal efficiency (>90%) has been observed in 5 h ball-milled Bi_2WO_6 in comparison with the efficiency of unmilled Bi_2WO_6 (34%) under 15 h UV light irradiation. This may be because ball milling reduced the size and increased the surface area of Bi_2WO_6. The adsorption and the active site of the reaction increases due to ball milling, which enhanced the performance of photocatalyst by degrading RHB (up to 90% in 15 h). After every 2 h, the absorption intensity decreased, showing the change in concentration of the dye molecule. As time increased, the blue shift in the graph was observed. Blue shift observed in the spectra was because of N-de-ethylation of RHB [42,43]. This led to the colour change of RHB from pink to pale green. The temporal evolution of RHB absorption spectra in the presence of 5 h ball-milled Bi_2WO_6 represents the pathway of degradation of RHB; (a) RHB, (b) N,N-diethyl-N-ethyl rhodamine, (c) N-ethyl-N-ethyl rhodamine, (d) N-ethyl rhodamine and (e) rhodamine. The hypsochromic shift in RHB has already been reported in the literature [44,45], where TiO_2/SiO_2 composite was used as photocatalyst for RHB. The degradation efficiency shown in figure 4d was calculated from the formula:

$$\eta = \left(\frac{A_0 - A_t}{A_0}\right) \times 100.$$

The reaction rate constant was calculated and presented in figure 4e, considering the reaction to be first order. To get a better understanding of kinetic reaction, the experimental data were fitted by pseudo-first-order model. The equation for calculation is as follows:

$$\ln\left(\frac{A_0}{A_t}\right) = -K_{app}t,$$

where K_{app} is the apparent first-order rate constant.

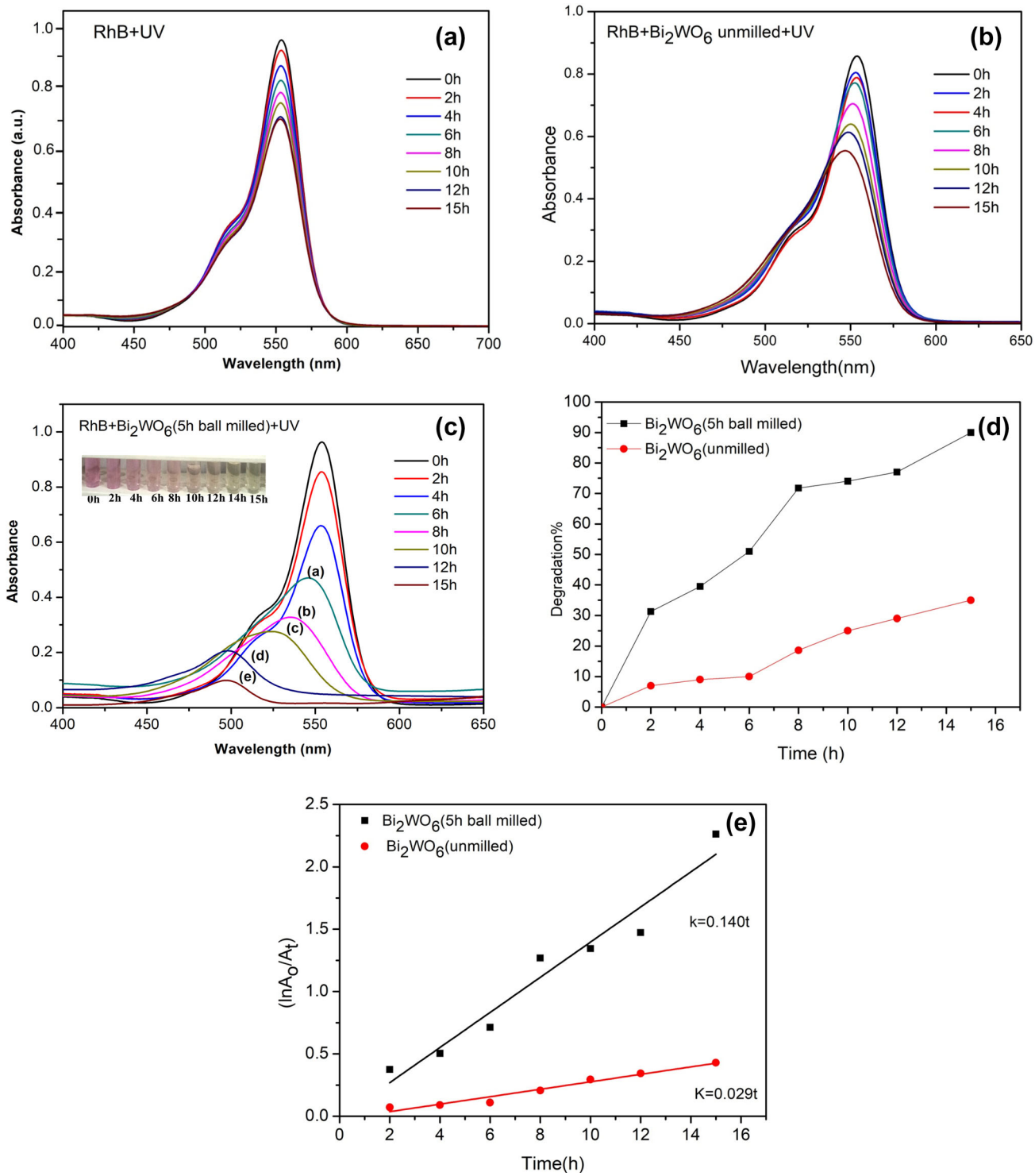

Figure 4. The photocatalytic activity of (**a**) RHB in the absence of photocatalyst, (**b**) unmilled, (**c**) 5 h milled, (**d**) degradation efficiency and (**e**) reaction rate constant of Bi_2WO_6 on RHB up to 15 h UV irradiation.

3.4 *Degradation of MB*

The photocatalytic performance of Bi_2WO_6 catalysts was evaluated by the degradation of MB exposed to UV light. There was minimal degradation of MB observed in 8 h of UV irradiation in the absence of catalyst due to its higher stability. The photocatalytic activity of unmilled Bi_2WO_6 and 5 h ball-milled Bi_2WO_6 against MB is shown in figure 5a and b, net UV irradiating time was 8 h, and the absorption intensity was measured. The observed absorbance peak positioned at 664 nm was monitored after every 1-h interval. The results show that the unmilled Bi_2WO_6

shows low activity (23%) against degradation of MB after 8 h, whereas 5 h ball-milled Bi_2WO_6 gave relatively higher efficiency (49%). The degradation activity of MB did not improve increasing the irradiation time beyond 8 h of irradiation time. Ball milling of Bi_2WO_6 enhanced its photocatalytic activity. The difference in photocatalytic activity may relate to UV light absorption properties, the separation efficiency of photogenerated electrons and holes, and efficient charge transfer. The degradation efficiency and rate constant of the photocatalyst is displayed in figure 5c and d.

3.5 *Proposed mechanism*

From the literature we know that ethanol and BQ are used as the scavenger of $OH^{\bullet}$ and superoxide ($^{\bullet}O^{2-}$) respectively, whereas KI is an efficient scavenger to both $^{\bullet}OH$ and photoexcited h^+ [46,47]. The investigation report of ethanol, KI and BQ is done by Wang *et al* [48], which showed that ethanol does not have any effect on the photocatalytic degradation of RHB, whereas KI and BQ reduce the photocatalytic degradation of dye. This result shows the dominance of h^+ and $^{\bullet}O^{2-}$ and negligible role of $^{\bullet}OH$ in the dye degradation. Under the UV light irradiation, Bi_2WO_6 was excited and produced the photogenerated charge carriers. The photogenerated holes at the valence band then react with water to produce $OH^{\bullet}$ radical. The formed $OH^{\bullet}$ on the surface of semiconductors is a powerful oxidizing agent. The anionic superoxide radical (O_2^-) is produced due to the reaction between electron in conduction band and oxygen. The superoxide radical gets protonated, forming hydroperoxyl radical ($HOO^{\bullet}$). Both oxidation and reduction process takes place on the surface of the photoexcited photocatalyst [49–51]. Primarily, all the four established species with a photogenerated hole (h^+), hydroxyl ($OH^{\bullet}$) radical, superoxide anion radical ($^{\bullet}O^{2-}$) and electron (e^-) are active during the photocatalytic processes, shown in figure 6.

The conduction band and the valence band potential plays a vital role in the explanation of photocatalytic reaction. The hybridized O 2p and Bi 6s states form the top of valence band and the W 5d states form the bottom of

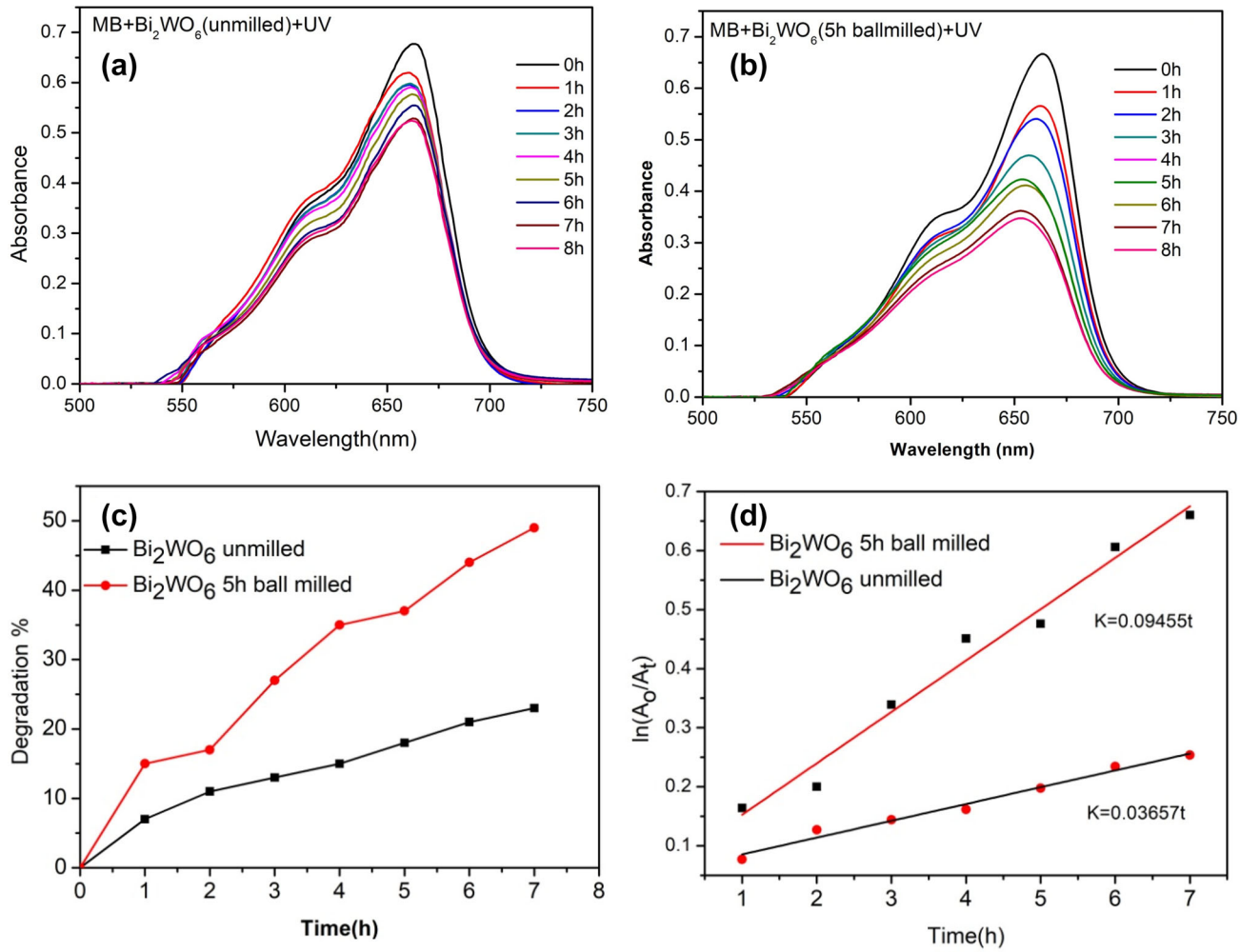

Figure 5. Photocatalytic activity of (**a**) unmilled Bi_2WO_6, (**b**) 5 h milled Bi_2WO_6, (**c**) degradation efficiency and (**d**) reaction rate constant of Bi_2WO_6 on MB up to 7 h UV irradiation.

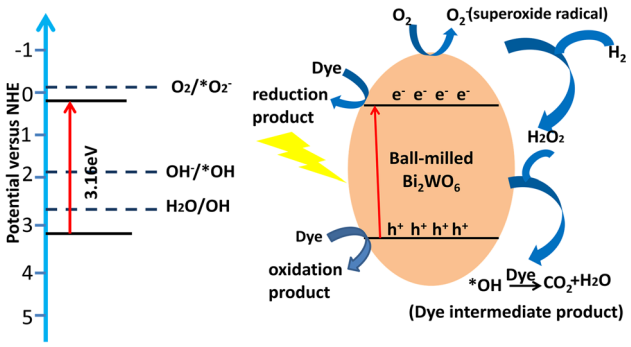

Figure 6. Pictorial representation of photocatalytic degradation of dye by Bi_2WO_6 powder.

conduction band in Bi_2WO_6 [52]. The conduction band and valence band have been calculated by Mullikan's equation [53], which is written as

$$E_{CB} = X - E_c - \frac{E_g}{2},$$

where X is defined as the arithmetic mean of electron affinity and ionization potential and is also called absolute electro-negativity of the catalyst and is reported to be 6.2 eV in the literature [54]. The E_c is the kinetic energy of free electrons of the hydrogen scale (4.5 eV), and E_g the optical energy bandgap of Bi_2WO_6 (ball milled) was calculated to be 3.16 eV [52]. The conduction band and valence band potential of ball-milled Bi_2WO_6 *vs.* normal hydrogen electrode was calculated to be 0.12 and 3.28 eV. The reaction between e^- and O_2 cannot proceed, as conduction band potential of Bi_2WO_6 is less negative than $O_2/^{\bullet}O_2^-$ (–0.13 V *vs.* normal hydrogen electrode). However, the conduction band potential might change in the solution as it changes with pH. In our photocatalytic reaction, the pH of the reaction was 7.5. This probably might have shifted the conduction band potential of Bi_2WO_6 towards negative compared to the calculated value. The increasing trend of conduction band with increase in pH has already been reported in the literature [55]. Thus, allowing the reaction between e^- and O_2 possible, with the production of $^{\bullet}O_2^-$. However, the valence band potential of ball-milled Bi_2WO_6 is higher compared to the redox potential of $OH^-/^{\bullet}OH$ and $H_2O/^{\bullet}OH$ (1.89 and 2.72 V *vs.* normal hydrogen electrode) [56]. Thus, the photoexcited h^+ can readily react with OH^- and H_2O to produce $^{\bullet}OH$ radicals. However, there is no $^{\bullet}OH$ found to be evolved. The possible reason for photoexcited h^+ cannot react with OH^-/H_2O to produce $^{\bullet}OH$ is that the photoexcited h^+ forms as Bi^{5+} oxidation state, and the redox potential of Bi^{5+}/Bi^{3+}, being +1.59 V *vs.* normal hydrogen electrode [57], is negative to those of $OH^-/^{\bullet}OH$ and $H_2O/^{\bullet}OH$, as reported in the literature [57]. Based on the results, we conclude that h^+ and $^{\bullet}O^{2-}$ are the dominant active species causing the RHB dye degradation, and $^{\bullet}OH$ plays a negligible role in the photocatalysis.

4. Conclusion

Bi_2WO_6 was successfully synthesized by using the solid-state reaction route followed by 5 h ball milling. The ball-milling technique reduced the crystallite size of the prepared sample from 100 to 34 nm. The prepared Bi_2WO_6 was employed as a catalyst in degrading RHB and MB. The 5 h ball-milled Bi_2WO_6 showed a remarkable degradation efficiency than unmilled Bi_2WO_6. Thus the experimental result confirmed that there exists a relationship between electron mobility and surface area. This had a significant effect on the catalyst's photocatalytic activity. The prepared catalyst is effective in degrading toxic dyes and cleaning wastewater from dye industries.

Acknowledgements

One of the author (SK) thanks the Department of Science and Technology, Government of India, for providing financial assistance through the WOS-A Fellowship (SR/WOS-A/CS-128/2018) to carry out the research work.

References

[1] Nestmann E R, Douglas G R, Matula T I, Grant C E and Kowbel D J 1979 *Cancer Res.* **39** 4412
[2] Chandler J E, Harrison C M and Canal A M 2000 *Theriogenology* **54** 261
[3] Youssef N A, Shaban S A, Ibrahim F A and Mahmoud A S 2016 *Egypt. J. Pet.* **25** 317
[4] Rabah M A 2008 *J. Waste Manag.* **28** 318
[5] Coolidge W D 1913 *Phys. Rev.* **2** 409
[6] Van Uitert L G and Preziosi S 1962 *Int. J. Appl. Phys.* **33** 2908
[7] Lecoq P, Dafinei I, Auffray E, Schneegans M, Korzhik M V, Missevitch O V *et al* 1995 *Nucl. Instrum. Methods Phys. Res. A* **365** 291
[8] Baccaro S, Borgia B, Cecilia A, Dafinei I, Diemoz M, Nikl M *et al* 1998 *Radiat. Phys. Chem.* **52** 635
[9] Treadaway M J and Powell R C 1975 *Phys. Rev.* **11** 862
[10] Chen W, Inagawa Y, Omatsu T, Tateda M, Takeuchi N and Usuki Y 2001 *Opt. Commun.* **194** 401
[11] Ehrenberg H, Weitzel H, Heid C, Fuess H, Wltschek G, Kroener T *et al* 1997 *J. Condens. Matter Phys.* **9** 3189
[12] Nagirnyi V, Feldbach E, Jönsson L, Kirm M, Lushchik A, Lushchik C *et al* 1998 *Radiat. Meas.* **29** 247
[13] Raj A E S, Mallika C, Sreedharan O M and Nagaraja K S 2002 *Mater. Lett.* **53** 316
[14] Garcia-Perez U M, Martinez-de La Cruz A and Peral J 2012 *Electrochim. Acta* **81** 227
[15] Sha Z, Sun J, Chan H S O, Jaenicke S and Wu J 2014 *RSC Adv.* **4** 64977
[16] Rahimi-Nasrabadi M, Pourmortazavi S M, Aghazadeh M, Ganjali M R, Karimi M S and Novrouzi P 2017 *J. Mater. Sci.: Mater. Electron.* **28** 3780

[17] López X A, Fuentes A F, Zaragoza M M, Guillén J A D, Gutiérrez J S, Ortiz A L *et al* 2016 *Int. J. Hydrog. Energy*. **41** 23312
[18] Amano F, Nogami K, Abe R and Ohtani B 2008 *J. Phys. Chem.* **112** 9320
[19] Amano F, Nogami K and Ohtani B 2009 *J. Phys. Chem.* **113** 1536
[20] Dai X J, Luo Y S, Zhang W D and Fu S Y 2010 *Dalton Trans.* **39** 3426
[21] Hu T, Li H, Zhang R, Du N and Hou W 2016 *RSC Adv.* **6** 31744
[22] Issarapanacheewin S, Wetchakun K, Phanichphant S, Kangwansupamonkon W and Wetchakun N 2016 *Ceram. Int.* **42** 16007
[23] Zhu S, Xu T, Fu H, Zhao J and Zhu Y 2007 *Environ. Sci. Technol.* **41** 6234
[24] Zhang L, Wang H, Chen Z, Wong P K and Liu J 2011 *Appl. Catal. B* **106** 1
[25] Yu J, Xiong J, Cheng B, Yu Y and Wang J 2005 *J. Solid State Chem*. **178** 1968
[26] Xia J, Li H, Luo Z, Xu H, Wang K, Yin S *et al* 2010 *Mater. Chem. Phys.* **121** 6
[27] Zhao G, Liu S, Lu Q and Song L 2012 *Ind. Eng. Chem.* **51** 10307
[28] Zhu Y, Wang Y, Ling Q and Zhu Y 2017 *Appl. Catal. B* **200** 222
[29] Xiao J, Dong W, Song C, Yu Y, Zhang L, Li C *et al* 2015 *Mater. Sci. Semicond. Process.* **40** 463
[30] Phuruangrat A, Dumrongrojthanath P, Ekthammathat N, Thongtem S and Thongtem T 2014 *J. Nanomater.* **2014** Article ID 138561
[31] Nobre F X, Junior W A G P, Ruiz Y L, Bentes V L I, Silva-Moraes M O, Silva T M C *et al* 2019 *Mater. Res. Bull.* **109** 60
[32] Maczka M, Hanuza J, Paraguassu W, Gomes Souza Filho A, Tarso Cavalcante Freire P and Mendes Filho J 2008 *Appl. Phys. Lett.* **92** 112911
[33] Fu H, Pan C, Zhang L and Zhu Y 2007 *Mater. Res. Bull.* **42** 696
[34] Frost R L, Duong L and Weier M 2004 *Spectrochim. Acta A* **60** 1853
[35] Kania A, Niewiadomski A and Kugel G E 2013 *Phase Transit.* **86** 290
[36] Mishra R K, Weibel M, Müller T, Heinz H and Flatt R J 2017 *Chimia* **71** 451
[37] Maczka M, Paraguassu W, Souza Filho A G, Freire P T C, Mendes Filho J and Hanuza J 2008 *Phys. Rev.* **77** 094137
[38] Tkalčević M 2016 *Doctoral dissertation* (University of Zagreb, Faculty of Chemical Engineering and Technology)
[39] Zhou Y, Zhang Y, Lin M, Long J, Zhang Z, Lin H *et al* 2015 *Nat. Commun.* **6** 1
[40] Loyalka S K and Riggs C A 1995 *J. Appl. Spectrosc.* **49** 1107
[41] Fujihara K, Izumi S, Ohno T and Matsumura M 2000 *J. Photochem. Photobiol. A* **132** 99
[42] Ma Y and Yao J N 1998 *J. Photochem. Photobiol. A Chem.* **116** 167
[43] Watanabe T, Takizawa T and Honda K 1977 *J. Phys. Chem. Lett.* **81** 1845
[44] Takizawa T, Watanabe T and Honda K 1978 *J. Phys. Chem. Lett.* **82** 1391
[45] López S M, Hidalgo M C, Navío J A and Colón G 2011 *J. Hazard. Mater.* **185** 1425
[46] Xian T, Yang H, Xian W, Chen X F and Dai J F 2013 *Prog. React. Kinet. Mec.* **38** 417
[47] Liu W, Wang M, Xu C and Chen S 2012 *Chem. Eng. J.* **209** 386
[48] Wang B, Yang H, Xian T, Di L J, Li R S and Wang X X 2015 *J. Nanomater* Article ID 146327
[49] Tanaka K, Padermpole K and Hisanaga T 2000 *Water Res.* **34** 327
[50] Gouvea C A, Wypych F, Moraes S G, Duran N, Nagata N and Peralta-Zamora P 2000 *Chemosphere* **40** 433
[51] Konstantinou I K and Albanis T A 2004 *Appl. Catal. B* **49** 1
[52] Fu H, Zhang L, Yao W and Zhu Y 2006 *Appl. Catal. B: Environ.* **66** 100
[53] Morrison S R 1980 *Electrochemical at semiconductor and oxidized metal electrodes* (New York: Plenum)
[54] Andersen T, Haugen H K and Hotop H 1999 *J. Phys. Chem. Ref. Data* **28** 1511
[55] Dung D, Ramsden J and Gratzel M 1982 *J. Am. Chem. Soc.* **104** 2977
[56] Tachikawa T, Fujitsuka M and Majima T 2007 *J. Phys. Chem.* **111** 5259
[57] Weast R C 1988 *Handbook of chemistry and physics* 1st edn (Boca Raton, Florida: CRC Press) p 69